Carbohydrate Polymers 257 (2021) 117570

Contents lists available at ScienceDirect

Carbohydrate Polymers

journal homepage: www.elsevier.com/locate/carbpol

Polysaccharide identification through oligosaccharide fingerprinting

Eshani Nandita [a], Nikita P. Bacalzo Jr. [a], Christopher L. Ranque [a], Matthew J. Amicucci [a,b], Ace Galermo [a], Carlito B. Lebrilla [a,b,*]

[a] Department of Chemistry, University of California, Davis, CA, USA
[b] Agricultural and Environmental Chemistry Graduate Group, University of California, Davis, CA, USA

ARTICLE INFO

Keywords:
Polysaccharide analysis
LC–MS
Food glycomics

ABSTRACT

The identification of polysaccharide structures in complex samples remains a unique challenge complicated by the lack of specific tools for polymeric mixtures. In this work, we present a method that depolymerizes polysaccharides to generate diagnostic oligosaccharide markers that are then analyzed by high performance liquid chromatography-quadrupole time-of-flight mass spectrometry (HPLC-QTOF MS). Rapid identification of food polysaccharides was performed by aligning the identified oligosaccharides with a library of oligosaccharide markers generated from standard polysaccharides. Measurements of standard and food polysaccharides were performed to obtain the contributions of the identified polysaccharides using percent peak coverage and angle cosine methods. The method was validated using a synthetic mixture of standard polysaccharides while the reproducibility was confirmed with experimental triplicates of butternut squash samples, where standard deviation was less than 3% for the relative abundance of oligosaccharides. The method was further employed to examine diverse set of food samples.

1. Introduction

Plant polysaccharides are the most abundant biomacromolecules found in nature, which serves as important structural components in the integrity of plant tissues (cellulose, hemicelluloses, pectins), as well as energy storage in the form of starch and fructans. Aside from their intrinsic biological functions, they are also central to a wide range of applications in nutrition and agriculture. Polysaccharides often have bioactive properties when consumed. For example, mushroom polysaccharides, which include chitin, α- and β-glucans, mannans, xylans, and galactans, are found to have antitumor and immunomodulating activities (Singdevsachan et al., 2016). Beyond food, polysaccharides are also components in therapeutics and nutraceutical products (Kothari, Patel, & Kim, 2018; Singdevsachan et al., 2016). Polysaccharides can also be used in monitoring agricultural products. Different stages in plant maturity have been associated with changes in polysaccharide compositions (Gross & Wallner, 1979; Redgwell, Melton, & Brasch, 1991; Yashoda, Prabha, & Tharanathan, 2005). Apples, for example, are considered ripe when they reach a low glucan and high polyuronide polysaccharide composition (Knee, 1973). Commercialization of polysaccharide products also employ polysaccharide composition analysis primarily for batch-to-batch product validation (Guan & Li, 2010; Jing et al., 2014). For example, the polysaccharide components in tea-based Chinese herbal medicines are monitored across batches to ensure all products contain the same composition in order to facilitate similar health benefits (Wang, Xian, Xi, & Wei, 2013). In such practices, the methods for polysaccharide analysis often requires tedious sample preparation and several instrument platforms, rendering them unsuitable for broad characterization of the different structural classes of polysaccharides.

There remains a clear and considerable need for rapid polysaccharide identification (Amicucci, Nandita, & Lebrilla, 2019). Plant polysaccharides have wide structural diversity as they can be composed of a variety of monosaccharides, linkage types, and degree of branching. As a result, there is no single method that can fully characterize polysaccharide compositions in complex matrices such as food. A traditional method for structural elucidation of plant polysaccharides involves nuclear magnetic resonance spectroscopy (Nie et al., 2013). However, this technique can only be performed on a highly concentrated and pure polysaccharide samples (Dourado, Cardoso, Silva, Gama, & Coimbra, 2006; Merkx et al., 2018). Plant polysaccharide composition analysis has also been performed by Fourier-transform infrared spectroscopy and applying extensive chemometrics (Coimbra, Gonçalves, Barros, & Delgadillo, 2002; Rocha, Delgadillo, Marcela, & Jana, 2003). In this

* Corresponding author at: University of California, Davis Department of Chemistry, One Shields Avenue Davis, CA, 95616, USA.
E-mail address: cblebrilla@ucdavis.edu (C.B. Lebrilla).

https://doi.org/10.1016/j.carbpol.2020.117570
Received 9 October 2020; Received in revised form 2 December 2020; Accepted 23 December 2020
Available online 5 January 2021
0144-8617/Published by Elsevier Ltd.

analysis, most of the diagnostic peaks are in the fingerprint region of the spectrum, specifically in the 500−1500 cm^{-1} range. Even with the use of chemometrics, significant overlap in the fingerprint region causes the analysis to increase in complexity as the number of polysaccharides in the mixture increases.

Mass spectrometry (MS) has been employed for the characterization of plant polysaccharides due to its high sensitivity and the ability to discriminate by mass-to-charge ratios. However, to be amenable to MS, polysaccharides must be depolymerized into oligosaccharides through either enzymatic or chemical processes. For example, enzymatically released plant oligosaccharides were used as diagnostic fingerprints to identify polysaccharides. This method used matrix-assisted laser desorption ionization-time of flight MS to characterize the oligosaccharides (Lerouxel, Choo, Se, Lerouge, & Pauly, 2002; Obel et al., 2009). However, the method lacks isomer separation of oligosaccharides which renders branching and linear structures indistinguishable. Additionally, a major drawback for enzymatic hydrolysis is that it requires the use of specific enzymes for each type of polysaccharide present. There is no single enzyme capable of universally cleaving all polysaccharides. Acid hydrolysis with gas-chromatography MS (GC–MS) of monosaccharides has also been used to predict the parent polysaccharide structures (Amicucci, Galermo et al., 2019; Doco, O'Neill, & Pellerin, 2001; Guadalupe, Martínez-Pinilla, Garrido, Carrillo, & Ayestarán, 2012; Xia, Wang, Sun, Liang, & Kuang, 2018). However, the monosaccharide arrangement information is lost during acid hydrolysis which renders the technique less suitable for overall polysaccharide identification. For example, both monosaccharide and linkage composition analyses cannot distinguish between amylose and cellulose, as both are (1→4)-linked glucose polymers that differs only in the anomeric character of the linkage. Hence, a complementary method for intact polysaccharide analysis is still needed.

In this research, we employed a recently developed chemical method for the degradation of plant polysaccharides into oligosaccharides (Amicucci et al., 2020). The method was optimized to be universal among plant polysaccharides. The resulting oligosaccharides were analyzed using liquid chromatography-mass spectrometry and were matched against a library of oligosaccharide fingerprints created from standard polysaccharides to determine the polysaccharide composition. Furthermore, the method was validated with commercially available polysaccharide standards and various food samples.

2. Materials and methods

2.1. Samples and materials

Sodium borohydride ($NaBH_4$), sodium hydroxide (NaOH), sodium acetate, glacial acetic acid, trifluoroacetic acid (TFA), hydrogen peroxide (H_2O_2), and iron(III) sulfate pentahydrate ($Fe_2(SO_4)_3 \cdot 5H_2O$) were purchased from Sigma-Aldrich (St. Louis, MO). Galactan, amylose, β-glucan, arabinan, xyloglucan, curdlan, arabinoxylan, lichenan, glucomannan, mannan, galactomannan, arabinogalactan and xylan were purchased from Megazyme (Bray, Ireland). Microcrystalline cellulose was purchased from ACROS Organics. Acetonitrile (ACN, HPLC grade) was purchased from Honeywell (Muskegon, MI). Formic Acid (FA) was purchased from Fisher Scientific (Belgium, UK). Porous graphitized carbon (PGC) solid phase extraction (SPE) plates were purchased from Glygen (Columbia, MD). Nanopure water (18.2 MΩ-cm) was used for all experiments. Yellow corn meal (*Zea mays*), wheat grass (*Triticum sp.*), whole grain oat cereal (*Avena sativa*), horseradish root (*Armoracia rusticana*), and coffee grounds (*Coffea arabica*) were purchased from the Davis Co-op (Davis, CA). Coconut (*Cocos nucifera*), jackfruit (*Artocarpus heterophyllus*), guava (*Psidium guajava*), yam leaves (*Dioscorea sp.*), bok choy leaves (*Brassica rapa*) were purchased from 99 Ranch Market (Sacramento, CA). Coffee grounds were brewed using conventional hot water extraction and the spent coffee grounds were used for polysaccharide analysis.

2.2. Food and polysaccharide sample preparation

All food samples were freeze-dried and ground to fine powder using Bead Ruptor Elite Bead Mill Homogenizer from Omni International (Kennesaw, GA). Stock solutions of polysaccharide standards and food were prepared at 10 mg/mL aqueous suspension and homogenized further with the bead homogenizer. Samples were heated in an oven at 100 °C for 1 h, and then 0.1 mL was transferred to reaction tubes. Aliquoted samples were dried by vacuum centrifugation prior to reaction.

2.3. Generation of representative oligosaccharides

Polysaccharides were depolymerized using an oxidative method optimized toward several polysaccharides (Amicucci et al., 2020). The treatment was performed on standard polysaccharides and food samples. Briefly, a reaction solution was prepared by mixing 95 mL of 40 mM sodium acetate buffer adjusted to pH 5 with glacial acetic acid, 5 mL of 30 % (v/v) hydrogen peroxide, and 3.2 mg $Fe_2(SO_4)_3 \cdot (H_2O)_5$. The reaction mixture was vortexed and added to each dried polysaccharide standards and food samples resulting in a final concentration of 1 mg/mL. To initiate the reaction, samples were incubated at 100 °C for 20 min. with a follow-up treatment with half of the reaction volume of 2 M NaOH to quench the reaction. Neutralization was performed by adding 61 μL of glacial acetic acid.

2.4. Reduction of oligosaccharides

Oligosaccharides were reduced by treatment with 1 M $NaBH_4$ for 1 h of incubation at 65 °C. Purification of oligosaccharides was performed using PGC cartridges. Cartridges were primed twice with 2 mL of 80 % ACN with 0.1 % (v/v) TFA and then conditioned twice with 2 mL of water prior to sample loading. After loading the entire reaction mixture, samples were washed five times with 2 mL of water. Elution of oligosaccharides was performed using 2 × 2 mL of 40 % ACN with 0.05 % (v/v) TFA. Vacuum centrifugation was used to dry the samples to completion.

2.5. High performance liquid chromatography-quadrupole time of flight mass spectrometry (HPLC-Q-TOF-MS) analysis

Samples were reconstituted in 100 μL of nanopure water before HPLC-Q-TOF-MS analysis. Analytical separation was carried out using an Agilent 1260 Infinity II HPLC coupled to an Agilent 6530 Accurate-Mass Q-TOF mass spectrometer operated in the positive mode. Chromatographic separation was performed on an analytical PGC column (Hypercarb, 5 μm particle size, 1 × 150 mm, Thermo Scientific). A binary gradient was employed and consisted of solvent A (3 % ACN/97 % H_2O with 0.1 % FA) and solvent B (90 % ACN/10 % H_2O with 0.1 % FA). A 45-min gradient with a flow rate of 0.150 mL/min was used for chromatographic separation: 3–25 % B, 0−15 min; 25 % B, 15−18 min; 25–99 % B, 18−30 min; 99 % B, 30−32 min; 99−3% B, 32−34 min; 3% B, 34−45 min. The mass spectrometer was run in positive mode and a reference mass with 922.0098 *m/z* was used for internal mass calibration. Drying gas temperature and flow rate were set to 150 °C and 11 L/min, respectively. Operation voltages for the fragment, skimmer, and octupole 1 RF were 175, 60, and 750 V, respectively. The acquisition rate was set to 0.63 spectra/second. For fragmentation, the linear function, Collision Energy = 1.45*(*m/z*)/100−3.5, was employed. Data obtained from the HPLC-QTOF MS were collected using Agilent MassHunter Workstation Data Acquisition version B.06.01. The acquired data were analyzed using Agilent MassHunter Quantitative Analysis version B.06.00. Oligosaccharide compositions were manually identified and annotated using tandem MS data, where neutral mass losses of the monosaccharides were used as basis for assigning monosaccharide class composition. The LC–MS profiles were annotated with the number of monosaccharides per monosaccharide class (Hexose or Hex, Pentose

or Pent, 4-*O*-Methylated Glucuronic Acid or GlcA-OMe) involved in the makeup of the identified oligosaccharide. The number of monosaccharides was represented as a subscript. For example, oligosaccharides containing a mixture of monosaccharide classes were labeled as Hex_nPent_m, where *n* represents the number of hexoses and *m* represents the number of pentoses. Thus, a monosaccharide composition of Hex_3-Pent indicated the presence of an oligosaccharide composed of 3 hexoses and 1 pentose resulting in an overall degree of polymerization (DP) of 4.

2.6. Measurement of similarity between chromatographic profiles

Two methods were employed to examine the similarity between the chromatographic profiles of standard and food polysaccharide samples. Peak coverage determines the percentage of oligosaccharide peaks observed in the food sample relative to the polysaccharide standard. Therefore, the higher the number of matched oligosaccharide peaks between the food and standard polysaccharide LC–MS profiles, the higher the percent peak coverage value for that polysaccharide.

A second approach involves a chemometric technique using the angle cosine method. In this method, the two chromatograms under investigation are treated as vectors of peak areas. The number of oligosaccharide peaks along with the corresponding area are included in the similarity computation. The angle cosine method was applied to measure the similarity between the two vectors which was calculated using Eq. (1):

$$r^{cos} = \frac{\sum_{i=1}^{n} x_i y_i}{\sqrt{\sum_{i=1}^{n} x_i^2 \sum_{i=1}^{n} y_i^2}} \quad (1)$$

where x_i and y_i refer to the chromatographic peak areas of oligosaccharide *i* between the two samples, respectively and *n* is the number of chromatographic peaks. Oligosaccharides were matched between two chromatograms using retention time values and compound masses. In this manner, a r^{cos} value of 0 indicates that there is no similarity between the two chromatograms while a value of 1 signifies that the two chromatograms are the same.

3. Results and discussion

The method employs oxidative degradation of polysaccharides followed by reduction of product oligosaccharides and purification before HPLC-QTOF MS analysis (Fig. 1). Depolymerization of polysaccharides to oligosaccharides was performed using a metal catalyst, $Fe_2(SO_4)_3$, and an oxidizing agent, H_2O_2, to produce hydroxyl radicals. Oligosaccharides were released and neutralized using NaOH and glacial acetic acid, respectively. The generated oligosaccharides were reduced using $NaBH_4$ to prevent chromatographic anomer separation during analysis. A final cleanup procedure employing solid phase extraction was performed to purify the oligosaccharide fraction. Reduced oligosaccharides were then analyzed by HPLC-QTOF MS.

3.1. Optimization of reaction conditions

To achieve the optimal reaction conditions, several parameters were optimized including the concentration of $Fe_2(SO_4)_3$ and H_2O_2, pH, reaction time and temperature. A substrate with a diverse monosaccharide and glycosidic linkage composition and a high degree of branching was chosen for the optimization of the reaction conditions. Xyloglucan, a heteropolysaccharide known to contain a β(1→4) glucose backbone with occasional α(1→6) xylose side-chains capped with galactose residues (Nishinari, Takemasa, Zhang, & Takahashi, 2007) was used for the optimization of the concentrations of $Fe_2(SO_4)_3$ and H_2O_2, pH, reaction time and temperature. The efficacy of the reaction was monitored by examining the total peak area and average DP of the generated xyloglucan oligosaccharides in the chromatogram.

Concentrations of $Fe_2(SO_4)_3$ and H_2O_2 were found to have significant roles on the overall efficiency of the oxidation reaction (Chan & Chu, 2003; Fischbacher, von Sonntag, & Schmidt, 2017). The optimal $Fe_2(SO_4)_3$ concentration was determined by comparing the total peak areas of the generated xyloglucan oligosaccharides with concentrations of 0.0065, 0.065, 0.65, 1.95, 6.5, and 65 μM. Maximum yield of oligosaccharides was observed at 65 μM of $Fe_2(SO_4)_3$ (Fig. 2A). The optimized $Fe_2(SO_4)_3$ concentration was then used to optimize for the concentration of H_2O_2. The H_2O_2 concentration was varied at concentrations of 0.06, 0.29, 0.58, and 1.16 M. Oligosaccharide yield was highest at 0.29 M of H_2O_2 (Fig. 2B). Correspondingly, the highest average DP of the generated product oligosaccharides was also observed at 0.29 M H_2O_2.

To optimize the buffer pH, a pH range between 2.0–12.0 was evaluated with the optimized concentrations of $Fe_2(SO_4)_3$ and H_2O_2. Previous studies on similar reactions revealed a strong pH dependency (Barb, Baxendale, George, & Hargrave, 1951; Weiss & Humphrey, 1949). The optimal pH for efficient oligosaccharide production was determined to be approximately 5.0 as shown in Fig. 2C. At pH 12.0, the average DP increased further. However, the total peak area of oligosaccharides was substantially lower. Under alkaline conditions, the

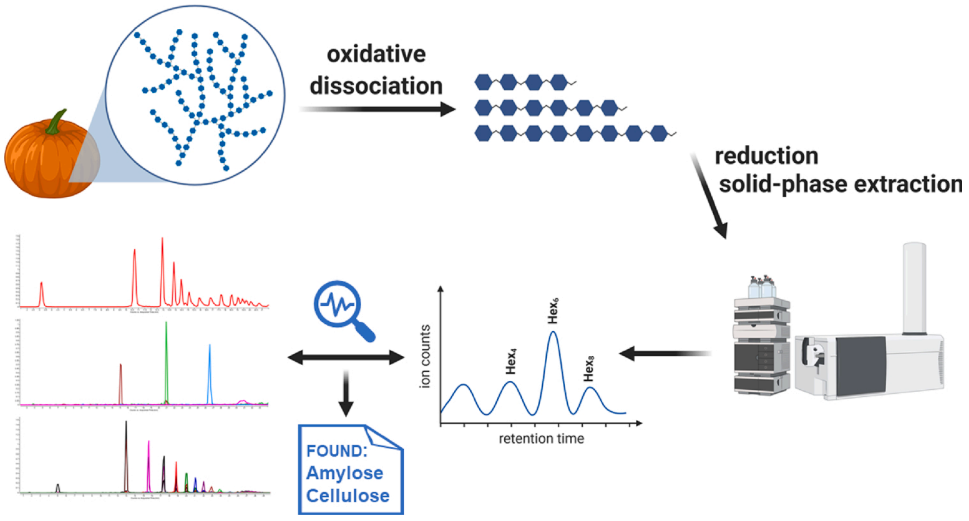

Fig. 1. Oxidative degradation of polysaccharides generates representative oligosaccharides which were reduced and purified for HPLC-QTOF MS analysis. Oligosaccharides identified in the LC–MS profile were aligned with the oligosaccharide fingerprint library to identify the corresponding parent polysaccharide.

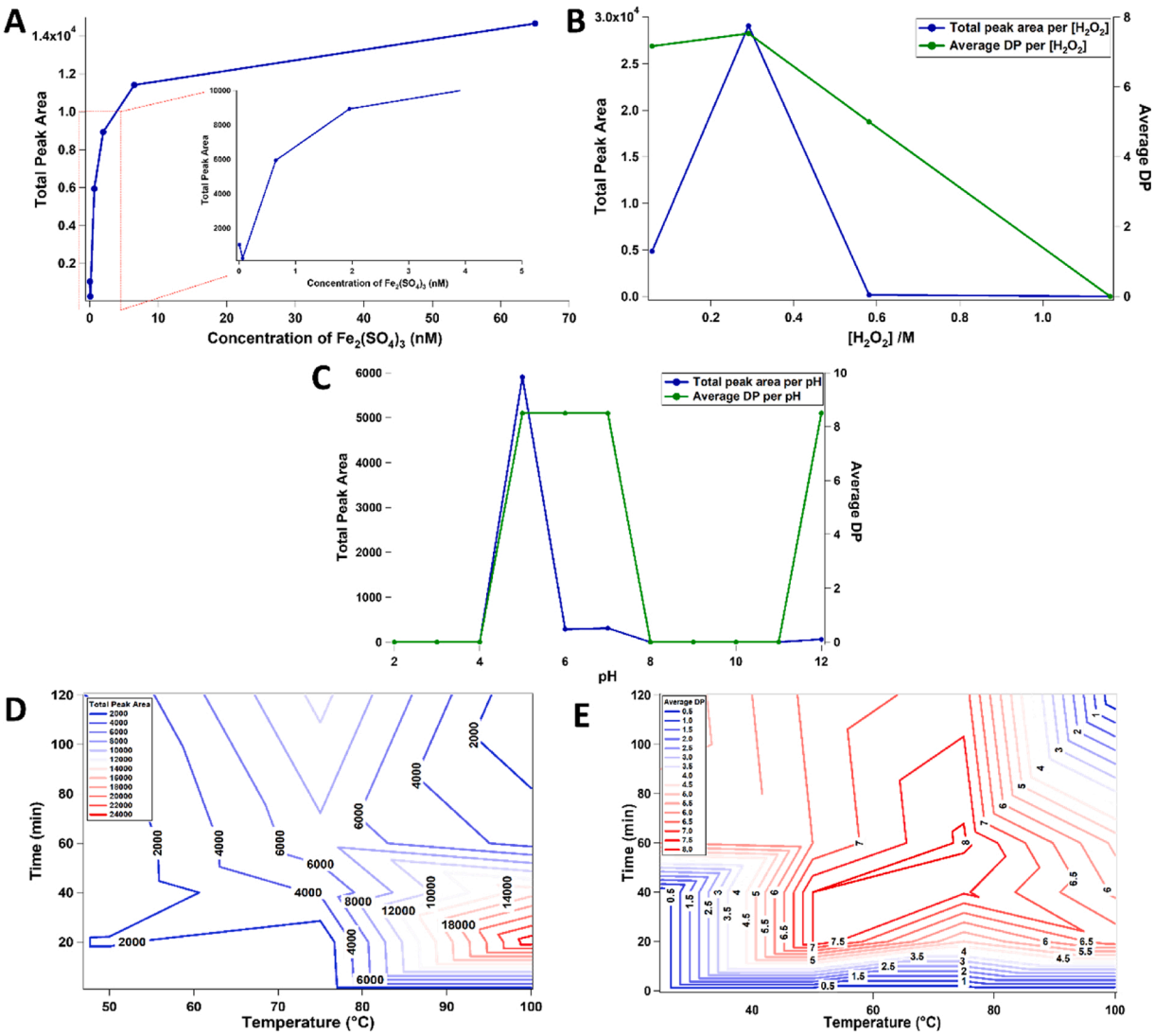

Fig. 2. Effective polysaccharide degradation was performed by optimizing several reaction parameters including the concentration of $Fe_2(SO_4)_3$ (**A**) and H_2O_2 (**B**), and pH (**C**). Time and temperature combination were also optimized to ensure high total peak area (**D**) and average DP (**E**) of the generated oligosaccharides.

decline in the progress of the oxidation reaction was attributed to the precipitation of $Fe(OH)_3$ (Fischbacher et al., 2017).

Reaction time and temperature were also determined to be important parameters in the efficiency of the oxidation reaction. The temperature was varied between 25 °C and 100 °C in increments of 25 °C while time was varied between 0 min and 120 min in increments of 20 min. Optimal yield was obtained at a temperature and time of 100 °C and 20 min (Fig. 2D). The highest average DP of product oligosaccharides in the chromatogram was observed at 75 °C after 60 min (Fig. 2E). However, the total yield at these conditions was substantially lower. Thus, a temperature of 100 °C and time of 20 min was chosen as the optimal condition for effective polysaccharide degradation.

Generation of hydroxyl radicals would yield not only glycosidic cleavage products but also other reaction side products such as oxidatively modified oligosaccharides. These side products, however, were not monitored because they are not used in the fingerprinting analysis. The reaction conditions were optimized to give the maximum yield of unmodified oligosaccharides since these products are more informative for deducing the parent polysaccharide structure.

3.2. Method validation

The optimized reaction conditions were used to generate a series of oligosaccharides that would fingerprint the corresponding plant polysaccharides. These oligosaccharides generated from commercially available polysaccharide standards were tabulated in Table A1, which includes their retention time, monoisotopic mass, oligosaccharide composition, and parent polysaccharide of each identified oligosaccharide. It was observed that each polysaccharide structure generated unique oligosaccharide markers that would be useful for a confident oligosaccharide identification in the sample matrix. Xylan, for example, produced oligosaccharides with methylated glucuronic acid residues, showing that the degradation reaction was able to preserve structural information of the parent polysaccharide. Most isomeric oligosaccharides with different linkage configurations are well-separated using the optimized LC method. PGC has been commonly used to effectively separate isomeric oligosaccharides (Amicucci et al., 2020; Ninonuevo et al., 2006; West, Elfakir, & Lafosse, 2010). Thus, a Hex_4 oligosaccharide from different parent polysaccharides, such as amylose, cellulose, galactan, and mannan, are all separated by the LC method. This highlights one of the advantages of this method in distinguishing closely related polysaccharide structures such as amylose and cellulose. Both polysaccharides gave distinct oligosaccharide profiles useful for identification. Additionally, isomeric oligosaccharides were also produced in more complex polysaccharides such β-glucan, wherein glucose units were attached as either β(1→4) or β(1→3) linkage, producing multiple

isomers for each DP, as high as DP of 6.

A validation step was performed to confirm the concept of fingerprinting polysaccharides using diagnostic oligosaccharides. The method was validated using a synthetic mixture of polysaccharide standards including arabinoxylan, xyloglucan, and amylopectin. The polysaccharides, mixed at equivalent ratios by mass, were reacted using the optimized conditions for oxidative degradation to produce representative oligosaccharides. The LC–MS oligosaccharide profile of a mixture of the three polysaccharides is shown in Fig. 3D. Peak annotation and matching were performed using the individual LC–MS profiles for arabinoxylan, xyloglucan, and amylopectin as shown in Fig. 3A–C, respectively.

LC–MS profiles of the individual standard polysaccharides were compared with the LC–MS profile of the mixture using the peak coverage method. The peak coverage value of a polysaccharide represents the percentage of oligosaccharide peaks observed from a mixture in relation to the oligosaccharide peaks observed from a pure polysaccharide solution. When compared to the pure sample, oligosaccharides in the mixture from amylopectin had a peak coverage value of 93 %, while xyloglucan and arabinoxylan had 45 % and 25 %, respectively. The discrepancy in the peak coverage values was ascribed to the wide distribution of molecular weights of the manufactured pure polysaccharides. There was an inherent difference in the molar ratio of the polysaccharides introduced into the oxidative degradation reaction. For this reason, peak coverage values cannot be used for quantitation. Rather, it only provides a metric of confidence for an identification. Polysaccharide quantitation is still an on-going research endeavor in our laboratory. However, the three polysaccharides in the mixture were successfully identified using oligosaccharide fingerprint information, which included monosaccharide composition, retention time, and monoisotopic mass. Thus, employing the oligosaccharide fingerprint library from pure polysaccharides for the identification of unknown polysaccharide compositions in a mixture was successfully validated.

3.3. Polysaccharide fingerprinting

The capabilities of the polysaccharide fingerprinting method were probed by analyzing unknown polysaccharide compositions of various foods. The optimized oxidative degradation method for polysaccharides was applied to food samples to generate representative oligosaccharides. Oligosaccharide fingerprints from food LC–MS profiles were matched with the library of oligosaccharide fingerprints generated from standard polysaccharides to confirm the corresponding polysaccharide composition. For example, if a Hex_6 at a retention time of 14.36 min was observed in the food LC–MS profile, it was inferred using the fingerprinting library that the Hex_6 was generated from amylose. Retention time shifts were corrected during peak alignment and library matching. Specifically, amylose oligosaccharides were used as retention time standards which were run on the instrument for every 12 sample injections. These served as retention time markers for the retention time correction.

In the current version of the oligosaccharide library, most

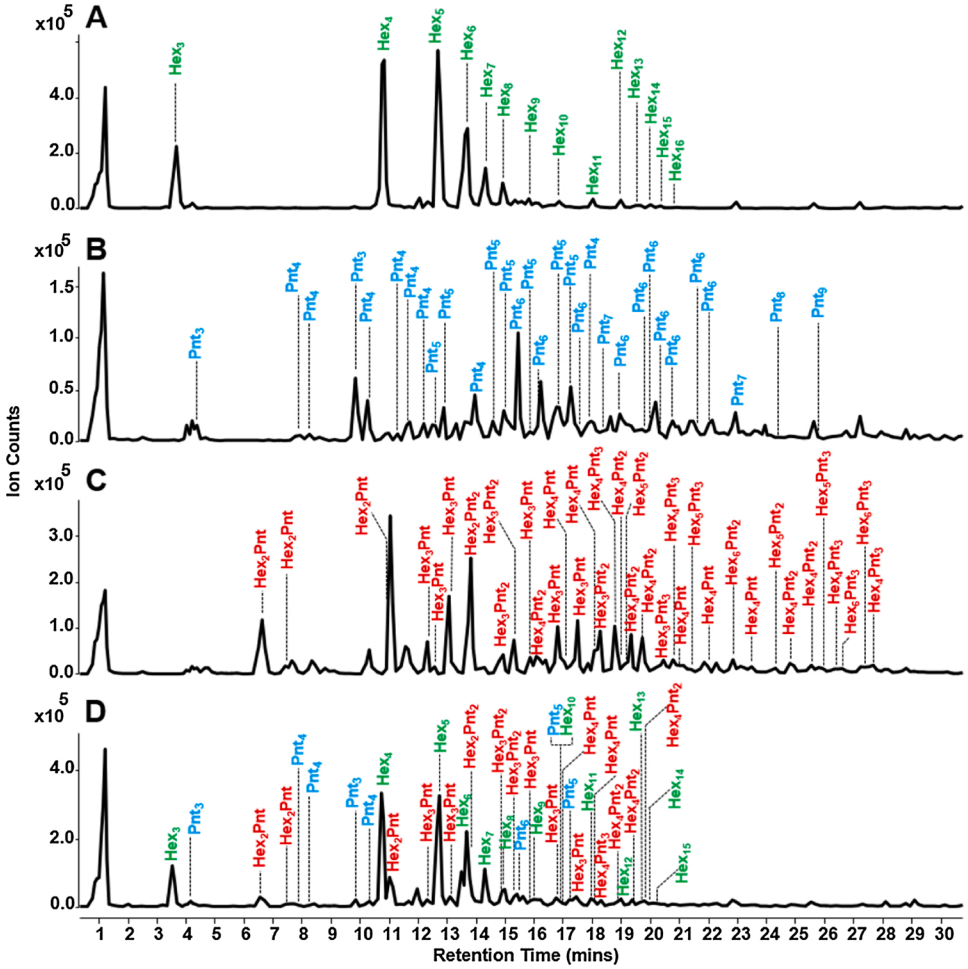

Fig. 3. Polysaccharide fingerprinting method validation was performed using a mixture of three polysaccharide standards. Annotated base peak chromatograms of the oligosaccharide profiles of amylopectin (**A**), arabinoxylan (**B**), xyloglucan (**C**), and the mixture (**D**) are illustrated. Using oligosaccharide fingerprints, all three polysaccharides were successfully identified in the mixture.

polysaccharides found in plants were included with the exemption of fructans, e.g. inulin and levan, and pectins, e.g. homogalacturonan and rhamnogalacturonan I. Pectins are one of the most abundant classes of plant polysaccharides present in the cell wall matrix, as well as the most complex ones. Fructans are also important plant storage carbohydrates in some plants. We are still optimizing the reaction conditions for these polysaccharides to get sufficient oligosaccharide signal from them. These will be included in the future reports. Additionally, we have added other non-plant polysaccharides in the library, such as curdlan and lichenan. Curdlan is mostly sourced from bacteria while lichenan is primarily sourced from lichens. These were included in the current polysaccharide library to provide more diverse oligosaccharides with both β(1→3)Glc and β(1→4)Glc linkages.

The reproducibility of the oxidative degradation reaction was determined using a food sample. Experimental triplicates of butternut squash were analyzed to ensure that the method generates reproducible LC–MS profiles and polysaccharide compositions. For each identified oligosaccharide, the retention time, oligosaccharide composition, and polysaccharide of origin are shown in Table 1. Average relative abundances and their corresponding standard deviations were also tabulated. Overall, standard deviation values were less than 3 % for relative abundances greater than 1 %, demonstrating reproducibility of the method for oxidative degradation of polysaccharides. Moreover, the polysaccharide composition of butternut squash correctly identified amylose and cellulose, which were in good agreement with literature (Phillips, 1946). Oligosaccharide peaks that were not identified using the library were binned until future assignments.

Table 1
Oxidative degradation method reproducibility was performed with experimental replicates ($n = 3$) of whole butternut squash sample. For relative abundances greater than 1%, standard deviations were calculated to be less than 3%, signifying the method reproducibility for polysaccharide degradation.

RT (min)	monosaccharide composition	relative abundance (%)	polysaccharide of origin
10.93 ± 0.01	Hex_4	17 ± 2	amylose
12.85 ± 0.06	Hex_5	14 ± 1	amylose
13.85 ± 0.02	Hex_6	9 ± 0	amylose
14.52 ± 0.02	Hex_7	7 ± 3	amylose
3.71 ± 0.03	Hex_3	5 ± 1	amylose
10.93 ± 0.01	Hex_3Pent	4 ± 1	*
12.89 ± 0.01	Hex_4Pent	4 ± 0	*
14.52 ± 0.02	Hex_8	4 ± 1	amylose
13.85 ± 0.02	Hex_5Pent	3 ± 0	*
3.68 ± 0.03	Hex_2Pent	2 ± 0	*
25.49 ± 0.02	Hex_5	2 ± 3	cellulose
19.82 ± 0.07	Hex_4	2 ± 3	cellulose
14.52 ± 0.02	Hex_6Pent	2 ± 1	*
15.2 ± 0.05	Hex_7Pent	2 ± 2	*
20.22 ± 0.01	Hex_{13}	1 ± 1	amylose
18.42 ± 0.04	Hex_{11}	1 ± 0	amylose
11.92 ± 0.03	Hex_3 #	1 ± 1	*
16.16 ± 0.04	Hex_9	1 ± 0	amylose
19.45 ± 0.06	Hex_{12}	1 ± 0	amylose
20.67 ± 0.1	Hex_{14}	1 ± 1	amylose
21.63 ± 0.004	Hex_{16}	1 ± 1	amylose

* Not present in the oligosaccharide fingerprinting library.
# Non-reducing oligosaccharide.

In addition to identification of the polysaccharides, an estimation of relative abundances was performed using similarity calculations between the LC–MS profiles of food and standard polysaccharides, specifically, the peak coverage and angle cosine methods. Identified polysaccharides that have high peak coverage values encompassed a greater number of oligosaccharide matches to the corresponding LC–MS profiles of standard polysaccharides. While peak coverage was an adequate method for running a quick measure of similarity by peak count, it did not consider peak areas. Thus, a chemometrics approach, employing the angle cosine method, was additionally used to measure similarity by treating the chromatograms from food and standard polysaccharides as vectors. The angle cosine method calculates r^{cos} values (similarity indices) using Eq. (1), where a value of 1 indicates high similarity and a value of 0 indicates low similarity between the two chromatograms. The calculated similarity indices along with the percent peak coverage values between the LC–MS profiles of food and standard polysaccharides are summarized in Table 2. These two metrics are expected to correlate but only to some extent since the calculations for each are very distinct from each other. While the peak coverage value is merely a peak counting metric, the cosine similarity considers the relative abundances of the peaks identified in both samples being compared.

An estimation of the abundance of the identified polysaccharides was performed using output values from the angle cosine method (Sun et al., 2014; Xu et al., 2009). Similarity indices were used to estimate which polysaccharides have the highest contribution to the polysaccharide composition of different food samples. The LC–MS profiles of identified polysaccharides that have high similarity indices resembled the profiles from standard polysaccharides. Therefore, such polysaccharides could have higher abundances in the sample relative to others. Validation of the concept was performed by evaluating of how well similarity indices conformed with the abundances of polysaccharides reported in literature as discussed below.

3.4. Food polysaccharide composition analysis

Oligosaccharide profiles of food samples including coconut flesh, yellow corn meal, jackfruit flesh, guava flesh, yam leaves, bok choy leaves, wheat grass, whole grain oatmeal cereal, horseradish root, and spent coffee grounds are shown in Fig. 4A–J. The results of the identified polysaccharides from food samples were compared to the profiles found in literature. However, literature values typically did not provide deep coverage in the polysaccharide analysis of most foods. In such cases, the reported monosaccharide composition analyses were compared with our findings from the polysaccharide fingerprinting method.

The LC–MS profile of the copra of coconut (*Cocos nucifera*) was determined to be composed of galactomannan, cellulose, mannan, arabinogalactan, β-glucan, arabinan, lichenan, and glucomannan (Fig. 4A). In literature, it was reported that the coconut flesh was composed of mannan-based polysaccharides, which were the highest in abundance (Khuwijitjaru, Pokpong, Klinchongkon, & Adachi, 2014). From our results, similarity indices from the angle cosine method for galactomannan and mannan were 0.586 and 0.494, respectively. Thus, the similarity indices were most likely directly proportional to the true abundance of the observed polysaccharides. Additionally, our method was capable of differentially identifying mannan, glucomannan, and galactomannan polysaccharides. Based on the results, it was evident that coconut flesh was mainly composed of mannan and galactomannan polysaccharides. Yellow corn meal (*Zea mays*), which is largely composed of corn starch, was expected to contain amylose polysaccharides (Gwirtz &

Table 2
Similarity indices between the LC–MS profiles of food and standard polysaccharides were examined for coconut flesh, yellow corn meal, jackfruit flesh, guava flesh, yam leaves, bok choy leaves, wheat grass, whole grain oatmeal cereal, horseradish root, and spent coffee grounds. Non-percentage values are similarity indices from the angle cosine method. Percentage values are peak coverage calculations.

	Similarity metrics between food samples and standard polysaccharides									
Standard Polysaccharides	Coconut flesh	Yellow corn meal	Jackfruit flesh	Guava flesh	Yam leaves	Bok choy leaves	Wheat grass	Whole grain oat	Horseradish root	Spent coffee grounds
Amylose	*	0.947, 95 %	0.976, 30 %	0.823, 63 %	0.978, 79 %	*	0.893, 47 %	0.863, 63 %	0.947, 32 %	0.995, 79 %
Mannan	0.494, 14 %	*	*	*	*	0.472, 14 %	*	0.349, 7 %	*	*
Cellulose	0.011, 33 %	*	0.705, 67 %	0.567, 100 %	0.239, 67 %	0.564, 67 %	0.593, 100 %	*	0.431, 100 %	0.011, 33 %
Curdlan	*	*	*	*	0.568, 33 %	*	*	*	0.568, 33 %	*
Lichenan	0.014, 3 %	*	*	*	*	*	*	*	*	*
β-Glucan	0.004, 4 %	*	0.178, 13 %	*	0.435, 22 %	*	*	*	0.555, 9 %	0.281, 22 %
Xylan	*	*	*	0.500, 4 %	*	*	0.500, 4 %	*	0.950, 17 %	*
Arabinoxylan	*	*	0.032, 2 %	0.485, 4 %	*	*	*	*	*	*
Galactomannan	0.586, 33 %	*	0.381, 7 %	*	0.202, 7 %	0.188, 15 %	*	*	*	0.233, 7 %
Glucomannan	0.068, 2 %	*	0.165, 2 %	0.165, 2 %	*	0.103, 3 %	*	*	*	*
Arabinogalactan	0.108, 5 %	*	*	*	*	*	*	*	*	0.319, 2 %
Arabinan	0.006, 4 %	*	*	*	0.006, 4 %	*	0.006, 4 %	0.006, 4 %	0.245, 13 %	*
Xyloglucan	*	*	*	0.658, 2 %	*	*	*	*	*	*

* Polysaccharide not present.

Garcia-Casal, 2014). Similarly, the results indicated that yellow corn meal was mainly composed of amylose as shown in Fig. 4B. The peak coverage was 95 % with a similarity index of 0.947, indicating a high abundance of amylose.

Jackfruit flesh (*Artocarpus heterophyllus*) polysaccharides were determined to be composed of amylose, cellulose, β-glucan, galactomannan, arabinoxylan, and glucomannan (Fig. 4C). Based on literature, jackfruit flesh was mainly composed of glucose, arabinose, and galactose monosaccharide components (Tan, Li, Lai, & Zhang, 2013; Zhu et al., 2017). While the literature results did not include polysaccharide compositions, the overall polysaccharide composition from the fingerprinting method matched with the reported monosaccharide compositions. Both amylose and cellulose were comparable to the standard profiles as represented by similarity indices of 0.976 and 0.705, respectively. Previous reports indicated a high abundance of glucose, (Tan et al., 2013; Zhu et al., 2017) which could be attributed to amylose and cellulose. Moreover, several Hex_nPent_m oligosaccharides were also identified. Based on the reported monosaccharide composition, (Tan et al., 2013; Zhu et al., 2017) arabinose could be one of the potential components of the Hex_nPent_m oligosaccharides.

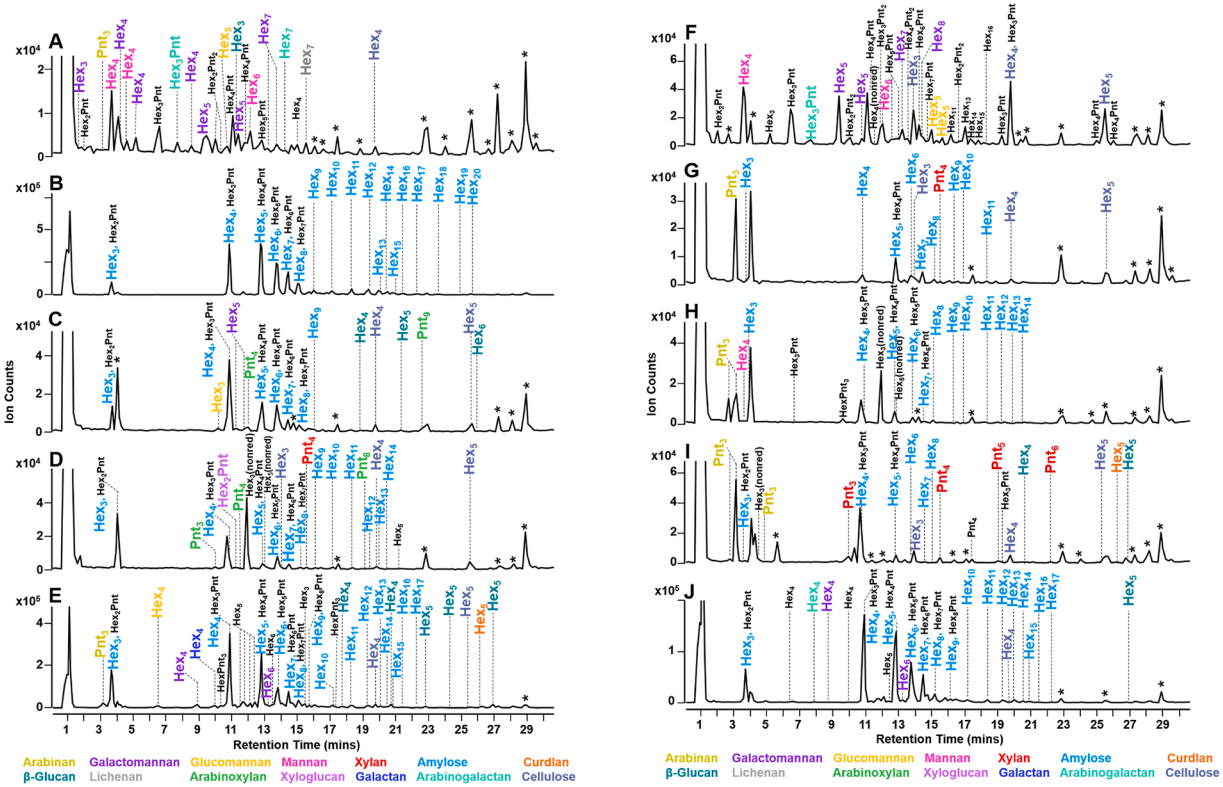

Fig. 4. Food polysaccharide fingerprinting was performed with coconut flesh (**A**), yellow corn meal (**B**), jackfruit flesh (**C**), guava flesh (**D**), yam leaves (**E**), bok choy leaves (**F**),wheat grass (**G**), whole grain oat cereal (**H**), horseradish roots (**I**), and spent coffee grounds (**J**). Corresponding polysaccharides are represented in a color-coded legend. Annotations of co-eluting peaks are separated by a comma. Oligosaccharides that are not present in the library were binned until future assignments. Non-oligosaccharide peaks were denoted with (*) (For interpretation of the references to colour in this figure legend, the reader is referred to the web version of this article).

Guava flesh (*Psidium guajava*) was composed of amylose, cellulose, arabinoxylan, xyloglucan, xylan, and glucomannan. A previous report found that guava flesh was primarily composed of glucose, xylose, and arabinose constituents, (Jiménez-Escrig, Rincón, Pulido, & Saura-Calixto, 2001) confirming the results from the fingerprinting method (Fig. 4D). Here, cellulose and amylose were the large contributors of the glucose content with similarity indices of 0.823 and 0.567, respectively. Additionally, one of the polysaccharides isolated from guava flesh in a previous study was characterized to contain a combination of 3-linked arabinose, 5-linked arabinose, 2,3,5-linked arabinose backbone with occasional glucose branching (Zhang et al., 2016). Thus, the binned Hex_nPent_m peaks could potentially correspond to the presence of a 'glucoarabinan' type polysaccharide.

Polysaccharides from yam leaves (*Dioscorea sp*.) are composed of β-glucan, cellulose, curdlan, galactomannan, amylose, and arabinan, as shown in Fig. 4E. There have been no report to our best knowledge of polysaccharides in yam leaves, however several studies have reported the presence of mannan in yam (Fu, Chen, & Lai, 2004; Myoda et al., 2006). Using our method, galactomannan was found with a peak coverage of 7% and a similarity index of 0.202. Based on this observation, galactomannan was present at a low abundance in yam leaves. Moreover, polysaccharide analysis of other types of yam have found β(1→3) linked glucose residues, (Yang, Wang, Li, & Yu, 2015) which was consistent with the presence of β-glucan and curdlan polysaccharides with similarity indices of 0.435 and 0.568, respectively.

The diverse composition of bok choy leaves (*Brassica rapa*) included cellulose, mannan, galactomannan, and glucomannan (Fig. 4F). Previous neutral monosaccharide analysis indicated a high abundance of glucose, galactose, and mannose residues (Vollendorf & Marlett, 1993). Therefore, it was consistent with the presence of cellulose, mannan, glucomannan, and galactomannan. The similarity indices for cellulose, mannan, glucomannan, and galactomannan were 0.564, 0.472, 0.103, and 0.188, respectively. This indicated that cellulose and mannan contributed to the high concentration of glucose and mannose. A significant amount of arabinose was previously reported, (Vollendorf & Marlett, 1993) which could be a possible component of the observed Hex_nPent_m oligosaccharides.

The polysaccharide composition of wheat grass (*Triticum sp*.) included cellulose, xylan, arabinan, and amylose (Fig. 4G). Previous studies reported xylan, arabinan, and β-glucan as significant polysaccharide components of wheat grass (Monono, Haagenson, & Pryor, 2012; Monono, Nyren, Berti, & Pryor, 2013). Literature from hydrolysis experiments determined high abundance of glucose, xylose, and arabinose residues (Zheng et al., 2006). The similarity indices of amylose, cellulose, xylan, and arabinan were 0.893, 0.593, 0.500, and 0.006, respectively. Thus, the largest contribution to the overall polysaccharide concentration originated from amylose, cellulose, and xylan. The results were similarly consistent with the previously reported compositions.

Whole grain oat (*Avena sativa*) cereal was composed of amylose, mannan, and arabinan as shown in Fig. 4H. Several reports indicated the presence of amylose, (Wang & White, 1994) arabinan, (Pronyk & Mazza, 2012) and β-glucans (Butt, Tahir-Nadeem, Khan, Shabir, & Butt, 2008; Wood, 2007). Using the fingerprinting method, amylose and mannan had the highest similarity indices, with 0.863 and 0.349, respectively. The results indicate that whole grain oat is largely abundant in amylose. Polysaccharides from horseradish (*Armoracia rusticana*) root included arabinan, β-glucan, curdlan, cellulose, xylan, and amylose (Fig. 4I). In literature, cellulose and starch were the most notable components of horseradish roots (Varo et al., 1984). Results from the polysaccharide fingerprinting method indicated a predominant presence of amylose and cellulose with similarity indices of 0.947 and 0.431, respectively. The percent peak coverage values were 32 % for amylose and 100 % for cellulose.

The polysaccharide fingerprinting method was also applied to spent coffee grounds (*Coffea arabica*) (Fig. 4J). Spent coffee grounds were composed of amylose, cellulose, β-glucan, galactomannan, and arabinogalactan. Monosaccharide composition analysis from literature indicated that glucose, galactose, and mannose were major residues present (Ballesteros, Cerqueira, Teixeira, & Mussatto, 2015). These results were in agreement with the corresponding polysaccharides from the fingerprinting method. The angle cosine similarity values for amylose, β-glucan, and arabinogalactan were 0.995, 0.568, and 0.319, respectively. Here, amylose and β-glucan are likely to be the more abundant polysaccharide structures which is comparable to the reported monosaccharide analysis (Ballesteros et al., 2015). The percent peak coverage values for amylose, β-glucan, and arabinogalactan were 79 %, 33 %, and 2 %, respectively.

In this set of samples, amylose and cellulose were the two most common polysaccharides identified. The results were expected as these samples were all plant-derived and some of them were rich in starch, as the case for yellow corn meal, while some were expected to be high in cellulose, such as wheat grass. Although curdlan and lichenan are both non-plant polysaccharides, they were detected in few samples but scored low in terms of peak coverage and peak area similarity. One reason might be that these oligosaccharides were from another mixed-linkage glucans similar to β-glucan, curdlan, and/or lichenan. These plant hemicelluloses can have a wide range of variety in terms of structure, and some of these polysaccharides may have shared some structural moieties. Overall, the analysis has shown the scarcity of information in literature regarding polysaccharide compositions in food. While most food composition analysis include monosaccharide, and some linkage information, very little is known regarding the intact polysaccharide structures. The method presented in this manuscript reveals up a more comprehensive view of carbohydrates in food.

4. Conclusions

We have developed a method for determining the polysaccharide composition of food based on polysaccharide degradation and oligosaccharide fingerprints generated from polysaccharide standards. This method represented a substantial improvement to the slow and stepwise methods for polysaccharide analysis. The oligosaccharide fingerprinting method was validated using a synthetic mixture of standard polysaccharides comprising of xyloglucan, amylose, and arabinoxylan. Method reproducibility was confirmed with experimental triplicates of butternut squash samples, where the overall standard deviation values were calculated to be less than 3% for oligosaccharides with relative abundances greater than 1 %. Successful polysaccharide composition identification was performed for ten various food samples. The identified polysaccharide list was validated by comparison with the known compositions in literature. Similarity index from angle cosine method was proven to be consistent with previously reported polysaccharide compositions of food samples and demonstrated to be an effective measure of similarity between pure standard and food polysaccharide LC–MS profiles.

Conventional methods for polysaccharide analysis mostly rely on monosaccharide and linkage information to predict the polysaccharide structures in the sample, which often results in several predicted candidates of the parent polysaccharide structures (Pettolino, Walsh, Fincher, & Bacic, 2012). In contrast to previous techniques, the presented method is capable of differentially identifying polysaccharides in food matrices such as glucose polysaccharides including amylose, cellulose, curdlan, lichenan, and β-glucan, which would otherwise be rendered indistinguishable from monosaccharide composition data.

Extending the current polysaccharide fingerprinting method for quantitation of polysaccharides would require an orthogonal tool to measure the concentration of identified polysaccharides. In combination with the polysaccharide fingerprinting method, quantitation of polysaccharides using an LC–MS platform is currently being developed and will be the topic of future reports. The presented optimized oxidative method for polysaccharide degradation and the comprehensive library of oligosaccharide fingerprints will allow for a more targeted and rapid

workflow for profiling polysaccharides.

CRediT authorship contribution statement

Eshani Nandita: Conceptualization, Methodology, Investigation, Writing - original draft. **Nikita P. Bacalzo:** Data curation, Visualization, Writing - review & editing. **Christopher L. Ranque:** Investigation, Writing - review & editing. **Matthew J. Amicucci:** Conceptualization. **Ace Galermo:** Conceptualization. **Carlito B. Lebrilla:** Supervision, Conceptualization, Writing - review & editing.

Declaration of Competing Interest

The authors declare no competing financial interest.

Acknowledgements

Funding provided by the Mars, Incorporated is gratefully acknowledged.

Appendix A. Supplementary data

Supplementary material related to this article can be found, in the online version, at doi:https://doi.org/10.1016/j.carbpol.2020.117570.

References

Amicucci, M. J., Nandita, E., Galermo, A. G., Castillo, J. J., Chen, S., Park, D., … Lebrilla, C. B. (2020). A nonenzymatic method for cleaving polysaccharides to yield oligosaccharides for structural analysis. *Nature Communications, 11*(1), 1–12. https://doi.org/10.1038/s41467-020-17778-1

Amicucci, M. J., Galermo, A. G., Nandita, E., Vo, T. T. T., Liu, Y., Lee, M., … Lebrilla, C. B. (2019). A rapid-throughput adaptable method for determining the monosaccharide composition of polysaccharides. *International Journal of Mass Spectrometry, 438*, 22–28. https://doi.org/10.1016/j.ijms.2018.12.009

Amicucci, M. J., Nandita, E., & Lebrilla, C. B. (2019). Function without structures: The need for in-depth analysis of dietary carbohydrates [Review-article]. *Journal of Agricultural and Food Chemistry, 67*, 4418–4424. https://doi.org/10.1021/acs.jafc.9b00720

Ballesteros, L. F., Cerqueira, M. A., Teixeira, J. A., & Mussatto, S. I. (2015). Characterization of polysaccharides extracted from spent coffee grounds by alkali pretreatment. *Carbohydrate Polymers, 127*, 347–354. https://doi.org/10.1016/j.carbpol.2015.03.047

Barb, W. G., Baxendale, J. H., George, P., & Hargrave, K. R. (1951). Reactions of ferrous and Ferric Ions with hydrogen peroxide part I: The ferrous ion reaction. *Transactions of the Faraday Society, 47*, 462–500.

Butt, M. S., Tahir-Nadeem, M., Khan, M. K. I., Shabir, R., & Butt, M. S. (2008). Oat: Unique among the cereals. *European Journal of Nutrition, 47*(2), 68–79. https://doi.org/10.1007/s00394-008-0698-7

Chan, K. H., & Chu, W. (2003). The dose and ratio effects of Fe(II) and H2O2 in Fenton's process on the removal of atrazine. *Environmental Technology, 24*(6), 703–710. https://doi.org/10.1080/09593330309385606

Coimbra, M. A., Gonçalves, F., Barros, A. S., & Delgadillo, I. (2002). Fourier transform infrared spectroscopy and chemometric analysis of white wine polysaccharide extracts. *Journal of Agricultural and Food Chemistry, 50*(12), 3405–3411. https://doi.org/10.1021/jf020074p

Doco, T., O'Neill, M. A., & Pellerin, P. (2001). Determination of the neutral and acidic glycosyl-residue compositions of plant polysaccharides by GC-EI-MS analysis of the trimethylsilyl methyl glycoside derivatives. *Carbohydrate Polymers, 46*(3), 249–259. https://doi.org/10.1016/S0144-8617(00)00328-3

Dourado, F., Cardoso, S. M., Silva, A. M. S., Gama, F. M., & Coimbra, M. A. (2006). NMR structural elucidation of the arabinan from Prunus dulcis immunobiological active pectic polysaccharides. *Carbohydrate Polymers, 66*(1), 27–33. https://doi.org/10.1016/j.carbpol.2006.02.020

Fischbacher, A., von Sonntag, C., & Schmidt, T. C. (2017). Hydroxyl radical yields in the Fenton process under various pH, ligand concentrations and hydrogen peroxide/Fe (II) ratios. *Chemosphere, 182*, 738–744. https://doi.org/10.1016/j.chemosphere.2017.05.039

Fu, Y. C., Chen, S., & Lai, Y. J. (2004). Centrifugation and foam fractionation effect on mucilage recovery from Dioscorea (Yam) tuber. *Journal of Food Science, 69*(9), 471–477.

Gross, K. C., & Wallner, S. J. (1979). *Degradation of cell wall polysaccharides during tomato fruit ripening'* (pp. 117–120).

Guadalupe, Z., Martínez-Pinilla, O., Garrido, Á., Carrillo, J. D., & Ayestarán, B. (2012). Quantitative determination of wine polysaccharides by gas chromatography-mass spectrometry (GC-MS) and size exclusion chromatography (SEC). *Food Chemistry, 131*(1), 367–374. https://doi.org/10.1016/j.foodchem.2011.08.049

Guan, J., & Li, S. P. (2010). Discrimination of polysaccharides from traditional Chinese medicines using saccharide mapping-enzymatic digestion followed by chromatographic analysis. *Journal of Pharmaceutical and Biomedical Analysis, 51*(3), 590–598. https://doi.org/10.1016/j.jpba.2009.09.026

Gwirtz, J. A., & Garcia-Casal, M. N. (2014). Processing maize flour and corn meal food products. *Annals of the New York Academy of Sciences, 1312*(1), 66–75. https://doi.org/10.1111/nyas.12299

Jiménez-Escrig, A., Rincón, M., Pulido, R., & Saura-Calixto, F. (2001). Guava fruit (Psidium guajava L.) as a new source of antioxidant dietary fiber. *Journal of Agricultural and Food Chemistry, 49*(11), 5489–5493. https://doi.org/10.1021/jf010147p

Jing, P., Zhao, S. J., Lu, M. M., Cai, Z., Pang, J., & Song, L. H. (2014). Multiple-fingerprint analysis for investigating quality control of Flammulina velutipes fruiting body polysaccharides. *Journal of Agricultural and Food Chemistry, 62*(50), 12128–12133. https://doi.org/10.1021/jf504349r

Khuwijitjaru, P., Pokpong, A., Klinchongkon, K., & Adachi, S. (2014). Production of oligosaccharides from coconut meal by subcritical water treatment. *International Journal of Food Science & Technology, 49*(8), 1946–1952. https://doi.org/10.1111/ijfs.12524

Knee, M. (1973). Polysaccharide changes in cell walls of ripening apples. *Phytochemistry, 12*(7), 1543–1549. https://doi.org/10.1016/0031-9422(73)80365-6

Kothari, D., Patel, S., & Kim, S. K. (2018). Anticancer and other therapeutic relevance of mushroom polysaccharides: A holistic appraisal. *Biomedecine & Pharmacotherapy, 105*(May), 377–394. https://doi.org/10.1016/j.biopha.2018.05.138

Lerouxel, O., Choo, T. S., Se, M., Lerouge, P., & Pauly, M. (2002). Rapid structural phenotyping of plant cell wall mutants by enzymatic oligosaccharide fingerprinting. *Plant Physiology, 130*, 1754–1763. https://doi.org/10.1104/pp.011965.Progress

Merkx, D. W. H., Westphal, Y., van Velzen, E. J. J., Thakoer, K. V., de Roo, N., & van Duynhoven, J. P. M. (2018). Quantification of food polysaccharide mixtures by 1H NMR. *Carbohydrate Polymers, 179*, 379–385. https://doi.org/10.1016/j.carbpol.2017.09.074

Monono, E. M., Haagenson, D. M., & Pryor, S. W. (2012). Developing and evaluating NIR calibration models for multi-species herbaceous perennials. *Industrial Biotechnology, 8*(5), 285–292. https://doi.org/10.1089/ind.2012.0018

Monono, E. M., Nyren, P. E., Berti, M. T., & Pryor, S. W. (2013). Variability in biomass yield, chemical composition, and ethanol potential of individual and mixed herbaceous biomass species grown in North Dakota. *Industrial Crops and Products, 41*(1), 331–339. https://doi.org/10.1016/j.indcrop.2012.04.051

Myoda, T., Matsuda, Y., Suzuki, T., Nakagawa, T., Nagai, T., & Nagashima, T. (2006). Identification of soluble proteins and interaction with mannan in mucilage of dioscorea opposita thunb. (Chinese yam tuber). *Food Science and Technology Research, 12*(4), 299–302. https://doi.org/10.3136/fstr.12.299

Nie, S. P., Wang, C., Cui, S. W., Wang, Q., Xie, M. Y., & Phillips, G. O. (2013). A further amendment to the classical core structure of gum arabic (Acacia senegal). *Food Hydrocolloids, 31*(1), 42–48. https://doi.org/10.1016/j.foodhyd.2012.09.014

Ninonuevo, M. R., Park, Y., Yin, H., Zhang, J., Ward, R. E., Clowers, B. H., … Lebrilla, C. B. (2006). A strategy for annotating the human milk glycome. *Journal of Agricultural and Food Chemistry, 54*(20), 7471–7480. https://doi.org/10.1021/jf0615810

Nishinari, K., Takemasa, M., Zhang, H., & Takahashi, R. (2007). Storage plant polysaccharides: Xyloglucans, Galactomannans, Glucomannans. In H. Kamerling (Ed.), *Comprehensive glycoscience: From chemistry to systems biology* (pp. 613–652). Elsevier.

Obel, N., Erben, V., Schwarz, T., Kühnel, S., Fodor, A., & Pauly, M. (2009). Microanalysis of plant cell wall polysaccharides. *Molecular Plant, 2*(5), 922–932. https://doi.org/10.1093/mp/ssp046

Pettolino, F. A., Walsh, C., Fincher, G. B., & Bacic, A. (2012). Determining the polysaccharide composition of plant cell walls. *Nature Protocols, 7*(9), 1590–1607. https://doi.org/10.1038/nprot.2012.081

Phillips, T. G. (1946). Changes in the composition of squash during storage. *Plant Physiology, 21*(4), 533–541.

Pronyk, C., & Mazza, G. (2012). Fractionation of triticale, wheat, barley, oats, canola, and mustard straws for the production of carbohydrates and lignins. *Bioresource Technology, 106*, 117–124. https://doi.org/10.1016/j.biortech.2011.11.071

Redgwell, R. J., Melton, L. D., & Brasch, D. J. (1991). Changes to pectic and hemicellulosic polysaccharides of kiwifruit during ripening. *II international symposium on kiwifruit* (pp. 627–634). Palmerston North: International Society for Horticultural Science.

Rocha, M., Delgadillo, I., Marcela, C., & Jana, C. (2003). Use of FT-IR spectroscopy as a tool for the analysis of polysaccharide food additives. *Carbohydrate Polymers, 51*, 383–389.

Singdevsachan, S. K., Auroshree, P., Mishra, J., Baliyarsingh, B., Tayung, K., & Thatoi, H. (2016). Mushroom polysaccharides as potential prebiotics with their antitumor and immunomodulating properties: A review. *Bioactive Carbohydrates and Dietary Fibre, 7*(1), 1–14. https://doi.org/10.1016/j.bcdf.2015.11.001

Sun, X., Wang, H., Han, X., Chen, S., Zhu, S., & Dai, J. (2014). Fingerprint analysis of polysaccharides from different Ganoderma by HPLC combined with chemometrics methods. *Carbohydrate Polymers, 114*, 432–439. https://doi.org/10.1016/j.carbpol.2014.08.048

Tan, Y. F., Li, H. L., Lai, W. Y., & Zhang, J. Q. (2013). Crude dietary polysaccharide fraction isolated from jackfruit enhances immune system activity in mice. *Journal of Medicinal Food, 16*(7), 663–668. https://doi.org/10.1089/jmf.2012.2565

Varo, P., Laine, R., Veijalainen, K., Espo, A., Wetterhoff, A., & Koivistoinen, P. (1984). Dietary fibre and avaialable carbohydrates in Finnish vegetables and fruits. *Journal of Agricultural Science in Finland, 56*, 49–59.

Vollendorf, N. W., & Marlett, J. A. (1993). Comparison of two methods of fiber analysis of 58 foods. *Journal of Food Composition and Analysis, 6*, 203–214. https://doi.org/10.1006/jfca.1993.1023

Wang, L. Z., & White, P. J. (1994). Structure and properties of amylose, amylopectin, and intermediate materials of oat starches. *Cereal Chemistry, 71*, 263–268. Retrieved from http://www.aaccnet.org/cerealchemistry/abstracts/1994/CC1994a52.asp.

Wang, Y., Xian, J., Xi, X., & Wei, X. (2013). Multi-fingerprint and quality control analysis of tea polysaccharides. *Carbohydrate Polymers, 92*(1), 583–590. https://doi.org/10.1016/j.carbpol.2012.09.004

Weiss, J., & Humphrey, C. W. (1949). Reaction between hydrogen peroxide and Iron salts. *Nature, 163*(4148), 691.

West, C., Elfakir, C., & Lafosse, M. (2010). Porous graphitic carbon: A versatile stationary phase for liquid chromatography. *Journal of Chromatography A, 1217*(19), 3201–3216. https://doi.org/10.1016/j.chroma.2009.09.052

Wood, P. J. (2007). Cereal β-glucans in diet and health. *Journal of Cereal Science, 46*(3), 230–238. https://doi.org/10.1016/j.jcs.2007.06.012

Xia, Y. G., Wang, T. L., Sun, H. M., Liang, J., & Kuang, H. X. (2018). Gas chromatography–mass spectrometry-based trimethylsilyl-alditol derivatives for quantitation and fingerprint analysis of Anemarrhena asphodeloides Bunge polysaccharides. *Carbohydrate Polymers, 198*(February), 155–163. https://doi.org/10.1016/j.carbpol.2018.06.066

Xu, S., Yang, L., Tian, R., Wang, Z., Liu, Z., Xie, P., … Feng, Q. (2009). Species differentiation and quality assessment of Radix paeoniae Rubra (Chi-shao) by means of high-performance liquid chromatographic fingerprint. *Journal of Chromatography A, 1216*(11), 2163–2168. https://doi.org/10.1016/j.chroma.2008.04.064

Yang, W., Wang, Y., Li, X., & Yu, P. (2015). Purification and structural characterization of Chinese yam polysaccharide and its activities. *Carbohydrate Polymers, 117*, 1021–1027. https://doi.org/10.1016/j.carbpol.2014.09.082

Yashoda, H. M., Prabha, T. N., & Tharanathan, R. N. (2005). Mango ripening - Chemical and structural characterization of pectic and hemicellulosic polysaccharides. *Carbohydrate Research, 340*(7), 1335–1342. https://doi.org/10.1016/j.carres.2005.03.004

Zhang, Z., Kong, F., Ni, H., Mo, Z., Wan, J. B., Hua, D., … Yan, C. (2016). Structural characterization, α-glucosidase inhibitory and DPPH scavenging activities of polysaccharides from guava. *Carbohydrate Polymers, 144*, 106–114. https://doi.org/10.1016/j.carbpol.2016.02.030

Zheng, Y., Pan, Z., Zhang, R., Wang, D., Labavitch, J., & Jenkins, B. M. (2006). Dilute acid pretreatment and enzymatic hydrolysis of saline biomass for sugar production. *2006 ASABE Annual International Meeting*.

Zhu, K., Zhang, Y., Nie, S., Xu, F., He, S., Gong, D., … Tan, L. (2017). Physicochemical properties and in vitro antioxidant activities of polysaccharide from Artocarpus heterophyllus Lam. pulp. *Carbohydrate Polymers, 155*, 354–361. https://doi.org/10.1016/j.carbpol.2016.08.074